Published in final edited form as:
Neuroimage. 2014 May 15; 92: 356–368. doi:10.1016/j.neuroimage.2013.12.044.

Developmental Stages and Sex Differences of White Matter and Behavioral Development through Adolescence: A Longitudinal Diffusion Tensor Imaging (DTI) Study

Daniel Simmonds[1,2,3,4,*], **Michael N. Hallquist**[1,2,5], **Miya Asato**[1,5,6], and **Beatriz Luna**[1,2,5,7]

[1]Laboratory of Neurocognitive Development, Western Psychiatric Institute, University of Pittsburgh and University of Pittsburgh Medical Center Pittsburgh, PA

[2]Center for the Neural Basis of Cognition, University of Pittsburgh and University of Pittsburgh Medical Center Pittsburgh, PA

[3]Medical Scientist Training Program, University of Pittsburgh and University of Pittsburgh Medical Center Pittsburgh, PA

[4]Center for Neuroscience, University of Pittsburgh and University of Pittsburgh Medical Center Pittsburgh, PA

[5]Department of Psychiatry, University of Pittsburgh and University of Pittsburgh Medical Center Pittsburgh, PA

[6]Department of Pediatrics, University of Pittsburgh and University of Pittsburgh Medical Center Pittsburgh, PA

[7]Department of Psychology University of Pittsburgh and University of Pittsburgh Medical Center Pittsburgh, PA

Abstract

White matter (WM) continues to mature through adolescence in parallel with gains in cognitive ability. To date, developmental changes in human WM microstructure have been inferred using analyses of cross-sectional or two time-point follow-up studies, limiting our understanding of individual developmental trajectories. The aims of the present longitudinal study were to characterize the timing of WM growth and investigate how sex and behavior are associated with different developmental trajectories. We utilized diffusion tensor imaging (DTI) in 128 individuals ages 8-28, who received annual scans for up to 5 years and completed motor and cognitive tasks. Flexible nonlinear growth curves indicated a hierarchical pattern of WM development. By late childhood, posterior cortical-subcortical connections were similar to adults. During adolescence, WM microstructure reached adult levels, including frontocortical, frontosubcortical and cerebellar connections. Later to mature in adulthood were major corticolimbic association tracts and

*Contact djs81@pitt.edu Address: Loeffler Building, 1st Floor 121 Meyran Ave, Pittsburgh, PA 15213 Phone: 412-383-8178.

connections at terminal gray matter sites in cortical and basal ganglia regions. These patterns may reflect adolescent maturation of frontal connectivity supporting cognitive abilities, particularly the protracted refinement of corticolimbic connectivity underlying cognition-emotion interactions. Sex and behavior also played a large role. Males showed continuous WM growth from childhood through early adulthood, whereas females mainly showed growth during mid-adolescence. Further, earlier WM growth in adolescence was associated with faster and more efficient responding and better inhibitory control whereas later growth in adulthood was associated with poorer performance, suggesting that the timing of WM growth is important for cognitive development.

Keywords

maturation; uncinate fasciculus; cingulum; prefrontal; inhibition; variability

1 Introduction

Adolescence is a unique period of development where continued refinements in brain structure and function parallel behavioral refinements in complex processing such as cognition and emotional regulation (Crone and Dahl, 2012; Spear, 2000). Brain volume, weight, regional functional specialization, and cortical folding are largely comparable to adults by early childhood (Armstrong et al., 1995; Giedd et al., 1999; Reiss et al., 1996). In contrast, processes associated with connections among neurons, such as synaptic pruning, dendritic arborization, and myelination continue through adolescence and beyond, speeding the integration of neurons and supporting mature network function (Huttenlocher, 1990; Pfefferbaum et al., 1994; Yakovlev and Lecours, 1967).

Histological studies have shown that most white matter matures early in development, including spinal roots and basic sensorimotor pathways (Yakovlev and Lecours, 1967). In contrast, prolonged development occurs in frontal, parietal, and temporal white matter (WM) (Huttenlocher, 1990; Yakovlev and Lecours, 1967), as well as connections to limbic regions such as the hippocampus (Benes et al., 1994). Cross-sectional studies using diffusion tensor imaging (DTI), which provide *in vivo* measurements of WM integrity, generally find that the development of WM extends over childhood and adolescence, particularly in fronto-temporal and limbic connections, such as the uncinate fasciculus, superior longitudinal fasciculus and the cingulum, as well as cortical-subcortical connections involving the frontal lobes and motor regions (Asato et al., 2010; Barnea-Goraly et al., 2005; Giorgio et al., 2008; Lebel et al., 2008; Schmithorst et al., 2002; Tamnes et al., 2010). While greatly informative, cross-sectional designs are limited in their power to detect age-related change, in part due to their inability to distinguish measurement error from true developmental change (Casey and Durston, 2006; Rogosa et al., 1982; Singer and Willett, 2003). In contrast, longitudinal studies in which DTI scans are obtained for individuals on several occasions provide incremental insight into growth trajectories over time and whether there are distinct (potentially nonlinear) periods of development (Burchinal and Appelbaum, 1991). To date, several longitudinal DTI studies of development have been published (Bava et al., 2010; Giorgio et al., 2009; Lebel and Beaulieu, 2011; Wang et al., 2012), all demonstrating

ongoing development of white matter during adolescence. However, these studies were limited in several important ways including: small sample sizes, which limits the power to detect developmental effects, and comparisons of only two time points, which undermine the ability to characterize growth trajectories. Finally, prior studies have typically examined a narrow age span, limiting developmental inferences about the timing of white matter maturation. Cross-sectional studies have suggested that several white matter pathways have nonlinear growth patterns (Hermoye et al., 2006; Lebel et al., 2012, 2008; Mukherjee et al., 2001), which may be mirrored by nonlinear growth in various motor and cognitive abilities (Kail, 1993; Luna et al., 2004). These findings suggest the intriguing possibility that there may be qualitatively distinct changes in WM and behavior associated with different stages of development.

In our previous cross-sectional DTI study (Asato et al., 2010), we identified regions exhibiting adolescent-specific immaturities in white matter by comparing 13–17 year-olds to 18– 30 year-olds. In the present longitudinal study, the primary aim was to use DTI methods to explore individual WM growth by including a large number of participants with three or more scans, and to use non-linear regression models in order to study the timing of regional/localized white matter maturation. We hypothesized a hierarchical maturation pattern first occurring in cortico-subcortical tracts, followed by cortico-cortical and corticolimbic tracts which would corresponds with the maturation of cognitive/behavioral performance.

We chose to focus on rate of change rather than mean levels previously examined in order to quantify growth. The rationale for this approach is similar to population growth charts, where a particular individual could be in the 25^{th} percentile and be mature, or in the 75^{th} percentile but still growing. Previous studies have inferred maturational status by rationally chosen, but arbitrary, mean-level based thresholds, such as 90% of the maximum (Lebel et al., 2008) or the mean of all subjects >18 years of age (Dosenbach et al., 2010). Both of these metrics are strongly influenced by the age range included in the study. However, by using growth rates, a less arbitrary threshold can be set: the point at which growth is no longer significantly different from zero represents maturity. Further, this approach allows the potential identification of multiple distinct stages of growth, with intermediate periods of slow/no growth. A similar methodological approach has been utilized to study nonlinear growth patterns using electroencephalography (EEG) (Thatcher, 1992), but remains unexplored in adolescence.

A second aim of our study was to examine sex differences in WM development. Initial cross-sectional studies indicate that male youth have larger white matter volumes with steeper increases in white matter growth and a more protracted maturation time course than females (De Bellis et al., 2001; Filipek et al., 1994; Lenroot et al., 2007). Our design was able to test more directly that sex differences in white matter are developmental in nature, by providing the ability to examine the effects of sex on stages of white matter growth.

Finally, we also aimed to examine associations between white matter development and motor/cognitive behavior, which has a protracted developmental course (Luna, 2009). Previous studies have shown correlations between cross-sectional age group developmental time courses of cognitive behavior and white matter growth, particularly in fronto-parietal

pathways (Liston et al., 2006; Nagy et al., 2004; Tamnes et al., 2012; Vestergaard et al., 2011); however, these studies have focused on brain-behavior correlations after controlling for linear effects of age, rather than examining how these correlations may change over development. Thus, we sought to characterize the association between motor/cognitive behavior and growth trajectories for individual tracts to better understand a brain structure basis of cognitive development. We hypothesized that associations between cognition and white matter growth would be evident in late-developing connections during adolescence when cognitive abilities are still maturing.

2 Methods

2.1 Study population

Participants included 128 typically developing individuals (61 male) ages 8-29 years (mean age at start of study = 14.9 ± 4.2). Each individual was scanned 1-5 times (1: 44, 2: 24, 3: 25, 4: 20, 5: 15) for a total of 322 scans. Of these scans, 81 (25.2%) were in children ages 8-12, 131 (40.7%) were in adolescents ages 13-17, and 110 (34.2%) were in adults ages 18 and up. When considering age at first scan, divided into child (36 male, 45 female), adolescent (64 male, 67 female) and adult groups (58 male, 53 female), there were no significant group differences by sex $\chi(2)^2 = 0.82$, $p = 0.66$); this remained true when considering only longitudinal data (2+ scans) (child - 14 male, 17 female; adolescent - 19 male, 16 female; adult - 9 male, 9 female; $\chi(2)^2 = 0.55$, $p = 0.76$; see Supplementary Table 1 for more details). For individuals with multiple scans, successive scans were separated by a minimum of 6 months (interscan interval: 1.1 ± 0.5 years).

All participants reported no past or current neurological or psychiatric disorders, no family history of these disorders in first-degree relatives and no contra-indications for scanning (such as claustrophobia or metal implants). All participants had IQ tested using the Wechsler Adult Intelligence Scale (WAIS) (Wechsler, 1981) and none had a full-scale intelligence quotient (FSIQ) of less than 80 (IQ at first visit: 107 ± 10). All participants gave informed consent and were compensated for their time. All experiments complied with the Code of Ethics of the World Medical Association (1996 Declaration of Helsinki) and were approved by the Institutional Review Board at the University of Pittsburgh.

2.2 DTI Acquisition

A 3T MR Siemens MAGNETOM Allegra scanner (Erlangen, Germany) with a standard circularity-polarized head coil was used to acquire diffusion-weighted images. Before the study scan participants were trained to remain still in a “mock” scan that provided auditory feedback about head motion. In addition, pillows were used to stabilize the head inside the head coil during study scans. Images were obtained using a spin-echo echo-planar imaging sequence; whole-brain coverage was achieved using 29 4mm-thick contiguous axial slices with an in-plane resolution of 1.56mm. Similar to other developmental DTI studies (Barnea-Goraly et al., 2005; Schmithorst et al., 2002), diffusion gradients were applied in 6 non-collinear directions. However, in the present study directions were averaged over 14 repetitions (b = 800 s/mm) in order to increase the signal-to-noise ratio. A minimally-diffusion weighted image (b0) was also acquired. The axial plane was aligned with the

anterior and posterior commissures to ensure consistency of image acquisition across subjects,.

2.3 DTI Preprocessing

Data were initially processed using DTIPrep software (Liu et al., 2010) to automatically identify and correct motion and scanner-induced artifacts. These procedures included identifying slice intensity artifacts, in which motion reduces the correlation of neighboring slices within a gradient, and gradient intensity artifacts, in which motion leads to a large variance from other gradients. None were detected. Further, data were all visually inspected by the first author on a slice-by-slice basis during analysis to identify intensity artifacts including banding and poor signal-to-noise ratio. Again, no artifacts were detected.

Data were then processed for analysis using the Oxford Centre fMRI of the brain Software Library (FSL) (Smith et al., 2004). Raw DICOM images from the scanner were converted to NIFTI format using *dcm2nii*. Following this, a mask was created using brain extraction ("*bet*") which segmented the brain from skull and other extracranial structures. Next, images were corrected for head motion and eddy current distortion ("*eddycorrec*t"). Finally, a tensor model was fit to the images ("*dtifit*"), in which each voxel was assigned 3 eigenvectors and eigenvalues, describing the water diffusion within the voxel. The standard measures of axial diffusivity (AD; diffusion along principal axis), radial diffusivity (RD; diffusion orthogonal to principal axis) and fractional anisotropy (FA; ratio of AD to RD, normalized on a scale from 0-1, with zero indicating isotropic diffusion and one indicating all diffusion in one direction) of each voxel were calculated for use in further analysis.

Additional processing for group analysis was performed using FSL's Tract-Based Spatial Statistics (TBSS) toolbox (Smith et al., 2006). For each measure (FA, AD, RD), images were eroded by zeroing out voxels on the border of the image to reduce registration artifact, resampled to 1×1×1mm, and normalized to the JHU-DTI81 template included with FSL. An FA "skeleton" was generated, by calculating a mean FA map across subjects and thresholding it at FA>0.2. Individual subject skeletons were then normalized to the mean skeleton. For RD and AD measures, these images were registered to the FA skeleton.

In order to best understand the spatial patterns of development, region-of-interest (ROI) analyses were performed in successively smaller steps. In the first step, all voxels were averaged to create an overall white matter skeleton average. Next, the skeleton was divided into two groups of white matter; core tracts based on the JHU-DTI81 atlas (Mori et al., 2005) and white matter regions adjacent to gray matter, which we termed regional termination zones (RTZs), based on the Harvard-Oxford cortical and subcortical atlases provided with FSL. The JHU core tracts were divided into five categories: 1) callosal tracts, including splenium, body, genu and tapetum; 2) cerebellar tracts, including inferior, middle and superior cerebellar peduncles; 3) projection tracts, including medial lemniscus, pontine crossing tract, corticospinal tract, cerebral peduncle, posterior thalamic radiation, internal capsule (subdivided into anterior, posterior and retrolenticular portions) and corona radiata (subdivided into anterior, superior and posterior portions); 4) association tracts, including external capsule, sagittal stratum, superior fronto-occipital fasciculus, superior longitudinal fasciculus and uncinate fasciculus; and 5) limbic tracts, including cingulum (subdivided into

cingulate and hippocampal portions) and fornix (subdivided into column/body and crescent). These regions are described in Table 1 and illustrated in Supplementary Figure 1.

Data were averaged over each category as well as averaged over the tracts within each category on an individual basis. The cortical RTZ's included: frontal, sensorimotor, parietal, occipital and temporal. Subcortical RTZ's included: cerebellum, basal ganglia, thalamus and medial temporal. Further, as studies have shown significant differences in DTI measures between hemispheres (Wahl et al., 2010), we separated all ROIs into homologous left and right regions to look at hemispheric differences.

2.4 Behavioral tasks

On a separate day within a month from the MRI study a subset of participants performed two oculomotor tasks: the visually-guided saccade task (VGS) and the antisaccade task (AS) as part of a larger longitudinal developmental study. The VGS task is a simple reflexive task where participants are instructed to look at a target appearing suddenly in the periphery to assess basic sensorimotor function. While accuracy reaches maturity early in development, saccade latencies continue to decrease until mid-adolescence (Fischer et al., 1997; Luna et al., 2004; Munoz et al., 1998). The AS task (Hallett, 1978) requires subjects to refrain from making a reflexive saccade to a suddenly appearing peripheral target and instead look in the opposite direction, a measure of cognitive control. The latency to initiate a correct response reaches adult levels by mid-adolescence, while the rate of correct inhibitory responses continues to improve through adolescence (Fischer et al., 1997; Fukushima et al., 2000; Klein and Foerster, 2001; Luna et al., 2004; Munoz et al., 1998). Participants fixated on a central point fixation cross for a variable interval (500, 2000, 4000 or 6000 ms), at which time the central fixation was extinguished and a peripheral target appeared. The peripheral target could appear in three to nine degrees left or right from the central fixation in one of four locations: far left, near left, near right or far right. The target remained on the screen for 1500ms, and subjects were to look at its mirror location after which the central fixation reappeared. Before the target appeared, participants were instructed by a colored fixation cross to make a saccade either towards (green/VGS) or away from (red/AS) the target. Each task contained 48 trials. A red fixation indicated an AS trial while a green fixation indicated a VGS trial. The VGS task was performed by 86 participants (42 male) in 215 sessions, with 45 (20.9%) in children, 86 (40%) in adolescence and 84 (39.1%) in adults. The AS task was performed by 82 participants (42 male) in 227 sessions, with 42 (18.5%) in children, 91 (40.1%) in adolescence and 94 (41.4%) in adults.

2.5 Behavioral preprocessing

Details of eye-movement data preprocessing are described elsewhere (Luna et al., 2004). In the VGS task, sessions were discarded if there were fewer than 32 correct trials available for analysis (e.g. discarded trials due to instrument error). Primary measures of interest were latency, measured as the time from cue onset to the end of the saccade, and variability, measured as the standard deviation of the latencies during the task. In the AS task, sessions were discarded if there were fewer than 32 combined correct and error trials available for analysis (discarded trials due to instrument error). Additionally, to ensure the task instructions were understood, sessions were discarded if the error rate was greater than the

mean population error rate plus two standard deviations (29 ± 21%). Inhibitory performance was calculated as the percent of trials with inhibitory errors.

2.6 Group analysis

Group analyses of DTI and behavioral data were performed using *R* (R Core Team, 2012), with figures made using the *ggplot2* package (Wickham, 2009). Longitudinal data were analyzed using mixed-effects regression (Pinheiro and Bates, 2000), via the *lme4* package. The equation for this model is $y_i = X_i\beta + Z_i b_i + \varepsilon_i$, where y represents the response variable, the subscript *i* denotes an individual, X is the matrix of fixed-effect regressors (e.g. age, sex, behavior, laterality), β is the vector of parameter estimates for the fixed effects, Z is the matrix of random-effects regressors (e.g. individual intercepts and slopes), *b* is the vector of random-effects coefficients (variances and covariances among the random effects are captured by the matrix **ψ**), and ε is the within-person measurement error. Fixed effects of age represent the average growth trajectory in the sample, whereas subject and time were included as random effects to account for individual variability around mean growth parameters (Singer and Willett, 2003).

Fixed effects of age were examined using a natural (cubic) spline model with knots at ages 13, 15.5, and 18, representing transitions into early adolescence, late adolescence and adulthood, respectively. We selected the same knots for all regions to maximize our ability to compare regions and decided that 3 knots was the best balance of allowing complex curves while minimizing data overfitting. The actual ages of the knots placement were modeled around the typical definition of adolescence (13-17) with an adolescent midpoint, allowing us to get a more accurate curve in adolescence that minimizes influence of data in late childhood and early adulthood, where sample data is lower.

Interactions were examined between age and sex/behavioral measures; as there was no effect found between sex and behavioral development, interaction of age, behavior and sex together was not examined. Given evidence of hemispheric differences in DTI measures (Wahl et al., 2010), hemispheric differences in WM development were examined. We did not examine association of handedness, as the majority of the sample is right-handed (n=120); however, prior work using DTI has shown that handedness and laterality are independent of each other (Gong et al., 2005).

For all models, regression diagnostics were performed on the skeleton average, and subjects were excluded from a model if their Cook's Distance exceeded n/4, a standard threshold for identifying outliers and high leverage cases that would distort regression parameters (Cook and Weisberg, 1982) (see Supplementary Table 1 for exclusion details). Improvements in model fit for more complex regression models (e.g., models that included age rather than intercept-only models) relative to simpler models were assessed using log-likelihood ratio tests (LRT). For example, models that included an age × sex interaction were compared to models without this term in order to assess the overall significance of this interaction. Corrections for multiple comparisons were made using Holm corrections (Holm, 1979) based on the groupings of regions (whole skeleton (1), tract groups (5), tracts (27), cortical RTZs (5), subcortical RTZs (4)); additionally, more lenient corrections were applied to tracts within a group if the tract group was significant (number of tracts in group vs. all

tracts). These corrections were applied to allow for detection of both global and local patterns.

In order to localize the stages of development during which growth occurred, as well as stages where time-varying factors had significant effects on WM development, rates of change in WM measures were examined via the first derivatives of the nonlinear growth model described above. To generate confidence intervals for rates of change over time, 1000 datasets of the same size as the empirical sample were generated from the model parameters using Markov Chain Monte Carlo (MCMC) draws from the posterior distribution; predictions were made at 0.1-year intervals and *p*-values were generated at these intervals using the empirical cumulative distribution function from the bootstrap-based null distribution. The age at which rate of change was no longer significantly different from the null ($p = 0.05$) was determined to be the point at which maturity was reached. For interactions among behavioral variables, slopes with the behavioral variable were calculated both for mean level and rate of change at each interval and compared to the null slopes at that interval. For analyses with categorical interactions (sex, hemispheric differences), Euclidean distances between categories were calculated at each interval and p-values again generated based on 1000 MCMC draws from the model. Raw and fitted data for each measure and ROI, as well as age and sex effects, are shown in Supplementary Figure 2.

3 Results

3.1 Format of results

Results below are presented for developmental effects and interactions with sex, behavior and hemispheric differences. For each model, average WM effects are first presented, followed by core WM categories, then individual tracts and RTZs. P-values are from omnibus chi-squared tests showing that a region has a significant main effect of or interaction with age. Ranges indicate the ages when growth or interactions are significant; multiple significant periods are separated by a forward slash.

3.2 Timing and stages of WM development

3.2.1 Fractional Anisotropy (FA)—Developmental effects were evident across the brain, with all tracts reflecting increases in FA with age with no regions showing significant decreases (See Figure 1 and Table 2). FA averaged across the WM skeleton continued to grow into mid-adolescence (range: 11.2-16.3, p=5.5e-06). In the core WM categories, projection tracts were mature by childhood (p=0.14), while other categories matured during adolescence, including callosal (range: 11.9-15.4, p=0.0062), cerebellar (range: 11.6-15.5, p=0.00046), limbic (range: 11.5-16.5, p=5.1e-09) and association (range: 8.2-16.7, p=4.4e-07).

Further, distinct trends in maturation were seen across individual tracts. Many tracts showed no effects of age indicating that maturation was complete by childhood; the majority of these tracts were middle and posterior projection tracts, connecting brainstem and subcortical regions to parietal and occipital cortex, including the medial lemniscus, pontine crossing tract, internal capsule (posterior and retrolenticular), corona radiata and posterior

thalamic radiation. Additionally, portions of the interhemispheric corpus callosum (genu, body, tapetum) were mature in childhood, as well as the superior frontal occipital fasciculus, (association tract connecting frontal, parietal and occipital regions), and the column/body portion of the fornix, (limbic tract connecting the septal nuclei to the hippocampus).

As indicated, the majority of white matter reached maturation during adolescence. Maturation during this time was seen for the remainder of the projection tracts, connecting brainstem and subcortical regions to frontal cortex, including the corticospinal tract (range: 10.1-15.8, p=7.1e-07), cerebral peduncles (range: 11.2-15.5, p=3.9e-05) and anterior internal capsule (range: 11.6-15.7, p=7.6e-05). Also reaching maturation during adolescence were the interhemispheric callosal fibers, with the posterior splenium maturing last (range: 11.9-15.3, p=0.0035), and all cerebellar white matter reached maturation during this time as well (superior – range: 11.8-14.9, p=0.0014; middle – range: 12-15.5, p=0.0039; inferior – range: 12.4-17, p=0.00013). Many long-distance cortico-cortical association tracts, including the sagittal stratum (range: 10.5-16.9, p=1.2e-07), external capsule (range: 8.2-13.7, p=7e-04) and superior longitudinal fasciculus (ranges: 11-14.1 / 14.9-16.6, p=0.00024), as well as cortico-hippocampal limbic tracts, including the crescent portion of the fornix (range: 13.1-16.4, p=0.0018) and the hippocampal portion of the cingulum (range: 11.2-16, p=1.7e-06), reached maturation during adolescence as well. Finally, RTZs began to mature during this time; this included subcortical RTZs in the thalamus (range: 8.2-16.3, p=1.1e-08), medial temporal lobes (range: 12.3-15.8, p=0.0089) and cerebellum (range: 12.7-15.8, p=0.044), as well as occipital cortical RTZs (range: 11.2-16.4, p=9.3e-08).

After adolescence and into adulthood there was continued growth in major frontal and limbic tracts that reached maturity at different ages. Most RTZs showed growth into the second decade of life (frontal (ranges: 10.7-16.3 / 19.1-20.9, p=4e-09), sensorimotor (ranges: 10.3-16.4 / 18.6-21.9, p=4.9e-11), parietal (ranges: 10.8-16.7 / 18.6-20.1, p=9.7e-10) and temporal (ranges: 10.7-17.2 / 18.6-20.1, p=1.1e-13) cortical and basal ganglia (ranges: 11.3-13.6 / 15.5-16.1 / 18.6-19.6, p=0.00011)). The cingulate portion of the cingulum (connecting frontal, parietal and hippocampal regions) (ranges: 8.2-13.9 / 18.7-20.8, p=3.3e-07) matured during this time as well. The uncinate fasciculus (connecting the orbitofrontal cortex, amygdala, hippocampus, and medial temporal lobes) (ranges: 12.7-13.3 / 19.7-28.2, p=0.0064) was the latest maturing region, with development continuing into the end of our sample age range (28.2 years). Further, it is notable that for all of these regions, there was an interim period during adolescence with no significant growth.

No interaction of age and hemispheric differences were found in the WM average or core WM categories (all p>0.1). In individual tracts, interaction was seen in the cingulate portion of the cingulum (range: 12.9-16, p=0.00022), tapetum (posterolateral) portion of the corpus callosum (range: 15.6-17, p=5.1e-06) and basal ganglia RTZ (range: 15.8-21.7, p=0.00012). These effects all reflected significant growth in the left hemisphere tracts (cingulum: p=0.00014, corpus callosum: p=0.028, basal ganglia: p=0.0087); during these periods, no significant growth was seen in these tracts in the right hemisphere.

3.2.2 Radial Diffusivity (RD)—RD decreases with development largely mirrored the FA findings described above (see Supplementary Table 2a). RD averaged across the WM

skeleton continued to grow into mid-adolescence (range: 8.2-16.1, p=2.3e-07). All five WM categories matured during mid-adolescence, and the timing of tracts and RTZs were mostly similar to those in FA, with some notable differences. The uncinate fasciculus matured in early adolescence (range: 11.7-13.5, p=0.001), while frontal (range: 11.6-16.2, p=6.6e-06) and temporal (range: 8.2-16.8, p=1.7e-13) cortical and basal ganglia (range: 12.1-15.9, p=0.00011) RTZs matured during mid-adolescence. In contrast, the occipital (ranges: 11.8-15.4 / 18.6-19.3, p=0.00073) and thalamic (ranges: 8.2-13.2 / 19.2-21.5, p=0.0021) RTZs matured during early adulthood. Further, there were no significant interactions of age and laterality on RD.

3.2.3 Axial Diffusivity (AD)—In contrast with FA, AD typically decreases with development, and the timing of developmental change is mainly orthogonal to FA and RD findings (see Supplementary Table 2b). AD averaged across the WM skeleton decreased into early adulthood (ranges: 9-13.4 / 15.3-18.7, p=0.00014). In the WM categories, limbic and callosal tracts did not change over development (p>0.05), association (range: 9.8-13, p=0.012) and cerebellar (range: 11.5-13.5, p=8.4e-05) tracts matured in early adolescence, and projection (ranges: 8.5-14 / 14.6-19.9, p=1.7e-07) tracts continued to decrease into adulthood. A majority of tracts and RTZs did not significantly change over development. Tracts showing decreases and maturing during adolescence include the posterior thalamic radiation (range: 11.3-13.5, p=0.00036), anterior corona radiata (range: 12-16.1, p=0.00036), superior fronto-occipital fasciculus (range: 11.4-16.4, p=7.3e-05), superior longitudinal fasciculus (ranges: 9.4-13.2 / 15.8-16.3, p=0.0021), and frontal (range: 12.1-16.4, p=0.0014), temporal (ranges: 10-13.4 / 15.7-16.1, p=0.001) and basal ganglia (range: 14.2-16.3, p=0.0094) RTZs. Tracts showing decreases and maturing in adulthood were mainly projection tracts, including pontine crossing tract (ranges: 12.6-12.7 / 18.4-21.3, p=0.0016), posterior internal capsule (range: 10-19.7, p=2.2e-09), superior corona radiata (range: 8.2-19.1, p=1.9e-10) and posterior corona radiata (range: 8.2-20.2, p=5.3e-14), as well as the middle cerebellar peduncle (ranges: 11.7-12.9 / 15.7-16.1 / 19.3-20.2, p=8.9e-05). In contrast, the fornix (column/body) showed developmental increase in AD, maturing in adulthood (ranges: 12-15.8 / 19.2-22.9, p=1e-04). The uncinate fasciculus also showed this pattern of developmental increase (range: 21.3-28.2, p=0.04), although the region did not reach significance after Holm correction.

There were only a few significant interactions of age and hemisphere on AD. In posterior thalamic radiation during late childhood (range: 12.2-12.5, p=0.00048), there was negative growth in the left hemisphere (p=5.4e-05), but not the right hemisphere (p=0.09). In the uncinate fasciculus during adolescence/early adulthood (range: 15.3-20, p=1.4e-06), there was negative growth in the right hemisphere (p=0.0089), but not the left (p=0.28). In the fornix (column/body portion) throughout development (ranges: 11.8-15.4 / 17.3-17.9 / 25-28.2, p=1.6e-05), there was positive growth in the left hemisphere in childhood/ adolescence (p=2.37e-06) and adulthood (p=0.00632), but not in the right during any period (all p>0.05).

3.3 Effects of sex on WM development

3.3.1 FA—Interaction of age and sex on WM measures is shown in Figure 2. Interaction was seen in the WM average (8.2-12.8 / 16.5-19.2, p=0.0033); these reflected significant growth rates in males (p=1.33e-15, 0.00147) during these periods, but not in females (p>0.3). In core WM categories, interaction was seen in cerebellar (range: 8.2-12.9, p=0.012) and limbic (ranges: 8.2-12.9 / 16.5-19.1, p=0.0019) regions, again reflecting growth in only males (all p<0.001); projection, callosal and association categories did not show significant interaction with sex (all p>0.05). Interactions in individual tracts and RTZs were seen in the superior cerebellar peduncle (efferent cerebellar pathways) (range: 8.2-13.2, p=0.00039), the crescent portion of the fornix (ranges: 8.2-11.3 / 13.5-15.1 / 16.3-19.9, p=0.0058), hippocampal portion of the cingulum (ranges: 8.2-13, p=0.0016), frontal RTZ (ranges: 8.2-12.6 / 16.3-19.7, p=0.0011), temporal RTZ (ranges: 8.2-12.8 / 16.5-19.3, p=0.0037), thalamus RTZ (ranges: 8.2-12.8 / 16.2-19.7, p=0.00026), and basal ganglia RTZ (range: 16.5-21.7, p=0.0064). In all cases, these differences reflected significant growth in males but not females (all p<0.05).

Interactive effects of age, sex and hemispheric differences were not significant in the WM average (p=0.6) or core WM categories (all p>0.026). Significant interaction was seen in several individual regions, including the splenium of corpus callosum (ranges: 12.7-13 / 15.9-16.1, p=0.0013), whereby males showed greater growth in only the left hemisphere relative to females. Interaction was also seen in the retrolenticular portion of the internal capsule (ranges: 15.8-19.3 / 22.8-28.2, p=0.0016); in the earlier period (15.8-19.3), males showed growth in the left hemisphere (p=0.0084), females showed decline in the left hemisphere (p=0.00015), and neither sex showed significant growth in the right hemisphere, while in the later period (22.8-28.2), males showed decline in the left hemisphere (p=0.0078) and no growth in the right hemisphere, while females showed no growth in the left hemisphere and decline in the right hemisphere (p=0.0022). Finally, in the basal ganglia RTZ, an interaction was seen (range: 15.9-28.2, p=9.9e-06), whereby males showed growth in the left hemisphere (p=6.9e-05) but not the right, and females showed no growth in both hemispheres.

3.3.2 RD—Sex differences in RD were more limited than those in FA, and included the core limbic group (ranges: 8.2-12.8 / 16.8-19.7, p=0.0034), and within that the cingulum (hippocampal portion) (range: 8.2-13, p=0.0046). Differences were also seen in the superior cerebellar peduncle (range: 8.2-13, p=0.0012). These all reflected growth decreases in males (all p<0.005) but not females.

Age, sex and laterality interaction were seen in two regions. In the medial temporal RTZ (range: 15.4-16.4, p=5.4e-08), there was significant negative growth in females in the left hemisphere (p=3.4e-07), and significant positive growth in males in the left hemisphere (p=0.0018); no effects were seen in the right. In the basal ganglia RTZ (range: 19.5-23.9, p=0.015), significant negative growth was seen in males in the left hemisphere only (p=0.0032).

3.3.3 AD—There were no sex differences in development of AD. There was an age, sex and laterality interaction in temporal RTZ (range: 19.5-26.9, p=0.003) demonstrating significant positive growth for males in the left hemisphere (p=0.0093).

3.4 Development of motor/cognitive behavior and interaction with WM development

Latency (mean reaction time [mRT]) (range: 11.6-12.8, p = 0.00021) and RT variability (standard deviation of RT [sdRT]) (range: 8.6-12.8 / 17.5-19.4, p = 1.6e-06) during the VGS task, and inhibitory errors during the AS task (range: 8.2-13.2 / 15.2-18.7, p = 4e-09), decreased across development (Supplementary Figure 3). There were no significant interactions between age and sex on any of the behavioral measures.

3.4.1 Latency—There were no significant effects of latency on FA and AD development. There were significant interactions with age, latency on RD (see Figure 3) in the WM average (p=0.048), and the core cerebellar group (p=0.0017), within that the middle cerebellar peduncle (p=0.00019). Association with mean RD level was seen during different periods in the WM average (22.4-23.7), core cerebellar group (8.2-11.4) and middle cerebellar peduncle (8.2-11.6 / 14.3-16.2), all representing slower responding with lower RD values. Associations with RD growth in WM average (19.1-23.7), core cerebellar (8.2-12.2 / 15.9-18 / 20.9-23.7) and middle cerebellar peduncle (8.2-12.3 / 15.9-18.5 / 21.1-23.7) showed a positive association (longer latency with higher RD) in children and adolescents, but that association flips in early adulthood. There were no significant hemispheric interactions with any of the measures.

3.4.2 RT variability—There was a significant effect of RT variability on FA development (see Figure 3) across the WM average (p = 0.00092). Associations were evident at minimally-overlapping stages of development for mean FA level (range: 8.2-11.2; 16.8-19.1; 23.6-23.7) and FA growth rates (range: 11.4-12.4; 15.6-16.1; 19.1-23.7). For mean FA levels, results indicated: 1) from 8.2-11.2, higher mean FA levels were associated with greater RT variability, 2) this pattern reversed from 16.8-19.1, such that higher mean FA levels were associated with lower RT variability, and 3) the pattern reversed again, with higher mean FA levels from 23.6-23.7 associated with higher RT variability. These results can be understood in the context of FA growth rates, with results demonstrating 1) higher growth rates of FA from 11.4-12.4 and 15.6-16.1 were associated with lower RT variability, and 2) this pattern reversed from 19.1-23.7, whereby higher FA growth rates were associated with higher RT variability. No significant interaction was seen for core WM categories, individual tracts or RTZs.

A similar finding was seen for RD in the WM average (mean range: 16.7-20.3, growth ranges: 15.4-17.8 / 19.9-23.7, p=0.01), as well as in the core cerebellar group (mean ranges: 14.4-15.8 / 17.6-19.7 / 23.4-23.7), growth ranges: 13.3-14.1 / 15.6-18.2 / 19.8-23.7, p=0.0049. These indicate the same pattern, such that growth in mid-late adolescence was associated with better performance, and growth in adulthood was associated with poorer performance; in the cerebellar WM, growth in early adolescence was also associated with poorer performance. There were no interactions of AD with RT variability or interactions of any of the measures with laterality.

3.4.3 Inhibitory errors—Inhibitory errors during AS were not significantly associated with WM development for all of the measures. However, there was a significant interaction of inhibitory errors and laterality on WM development for all measures, primarily in limbic connections (see Figure 4). For FA, core limbic WM (mean range: 17.2-21.6, growth range: 15.2-16.7, p=0.0034) showed interactions only in the left hemisphere, with higher FA growth in mid-adolescence (p=0.049) and higher mean FA levels in late adolescence/early adulthood (p=8e-04) associated with lower error rates. Within limbic WM, the cingulum (hippocampal portion) also showed interaction with inhibitory errors in the left hemisphere only (mean ranges: 12.8-14.3 / 16.9-21.4, growth ranges: 15-17.7 / 20.7-24.7, p=0.00088), demonstrating that higher mean FA levels were associated with higher error rates in early adolescence (p=0.0091) and lower error rates in late adolescence/early adulthood (p=0.017); similarly, higher FA growth in mid-late adolescence was associated with lower error rates (p=0.00024) and in early adulthood was associated with higher error rates (p=0.00056).

For RD, limbic associations were also seen in both portions of the fornix. In the column/body (mean range: 9.6-13.9, growth range: 12.7-15.4, p=0.0057), interactions only in the left hemisphere showed that higher mean RD levels in childhood/early adolescence (p=0.00086) and greater RD decreases in early-mid adolescence (p=0.01) were associated with lower error rates. In the crescent (mean ranges: 13.8-15.1 / 20.6-24.7, growth ranges: 18.3-20.9, p=0.013), higher mean RD levels in the right hemisphere in early adolescence were associated with lower error rates (p=0.016); in the left hemisphere, in early adulthood, higher mean RD levels (p=0.033) and higher RD growth (p=0.034) were associated with increased error rates. Similar interactions were also seen in the rostral internal capsule (p=0.0015) and the body of the corpus callosum.

For AD, significant interaction was seen in the column/body of the fornix (mean range: 9.5-13.7, growth range: 12.4-15.6, p=0.0014). In the left hemisphere only, higher mean AD levels (p=0.0054) and decreased AD growth (p=0.0036) in childhood and early adolescence were associated with lower error rates.

4 Discussion

4.1 Timing of white matter development: hierarchical maturation

To date, studies of white matter development have relied on cross-sectional designs (Asato et al., 2010; Barnea-Goraly et al., 2005; Giorgio et al., 2008; Lebel et al., 2008; Schmithorst et al., 2002; Tamnes et al., 2010) or repeated DTI measures at two time points (Bava et al., 2010; Giorgio et al., 2009; Lebel and Beaulieu, 2011; Wang et al., 2012), limiting the ability to characterize growth trajectories and make direct inferences about developmental change. The present longitudinal study included one to five annual data points for each subject, allowing us to apply mixed-effects regression to understand the timing and stages of WM development, which has not previously been examined. Results showed that for several late-maturing regions including those connected to prefrontal regions, distinct phases of growth were seen, with rapid growth in childhood, followed by a slowdown slowing of growth in early-middle adolescence and acceleration of growth again in late adolescence/early adulthood. This is consistent with postmortem studies in prefrontal cortex showing a late adolescent spurt of growth in synaptic density (Huttenlocher, 1990; Paus et al., 2008). While

discrete growth periods have been observed for in young children with EEG coherence (Thatcher, 1992), this is the first longitudinal identification of such stages during the adolescent period in WM maturation. This finding is key, as most studies only investigate simple linear, inverse or quadratic models of development and cannot identify discrete periods of WM development.

Topographically, results showed that many projection tracts integrating posterior cortical and subcortical structures to brain stem regions were largely mature by late childhood, whereas frontocortical and frontosubcortical WM connections grew through adolescence maturing approximately by 15-16 years of age. Growth continued into adulthood the second decade of life in major corticolimbic association tracts and regional termination zones (RTZs) in cortical and basal ganglia regions. Overall, these results agree with findings from cross-sectional and follow-up DTI studies (Asato et al., 2010; Barnea-Goraly et al., 2005; Bava et al., 2010; Giorgio et al., 2009, 2008; Lebel et al., 2008; Lebel and Beaulieu, 2011; Schmithorst et al., 2002; Tamnes et al., 2010; Wang et al., 2012). However, the present study extends these findings, allowing the detection of discrete periods of significant growth with interim periods of decreased growth.

Of the regions that were already mature in childhood, many play a role in basic sensorimotor function. The posterior thalamic radiation carries visual sensory information from the retina to the primary visual cortex via the thalamus, while portions of the internal capsule and corona radiata carry somatosensory information from the spinal cord and brainstem to the primary sensory cortex via the thalamus (Mori et al., 2005; Schmahmann and Pandya, 2006). These findings are consistent with the early maturation of basic sensorimotor function seen in prior studies (Luna et al., 2004), which is critical to support the later development of cognitive functions.

Many of the regions that mature in adolescence play a pivotal role in motor response preparation and executive function. For example, the superior longitudinal fasciculus connects frontal and parietal regions important for motor planning and initiation, spatial attention, working memory and language (Dosenbach et al., 2007; Sauseng et al., 2005; Schmahmann et al., 2007; Schmahmann and Pandya, 2006; Vincent et al., 2008). These findings are consistent with studies showing that executive and cognitive functions including response inhibition and working memory continue to mature into adolescence, when adult-level performance is reached (Bedard et al., 2002; Luna et al., 2004; Williams et al., 1999).

Growth in cortical and basal ganglia RTZs continued into adulthood. These results agree with post-mortem analysis of myelination has demonstrated studies showing a prolonged maturation of intracortical white matter (Yakovlev and Lecours, 1967). Specifically, we found that occipital based tracts matured in adolescence, while other cortical regions mature in adulthood, consistent with evidence of a posterior to anterior hierarchy in maturation of synaptic density and myelination (Huttenlocher, 1990; Petanjek et al., 2011; Yakovlev and Lecours, 1967). Further, late maturation was also seen in the basal ganglia, which forms loops with the cortex and is a key relay in cognitive and emotional processing (Middleton and Strick, 2000). Late maturation of these areas may suggest that a large cortical-subcortical network is critical for integrating cognition and emotion.

Further, growth of the uncinate fasciculus and cingulum also continues into the second decade of life. Both of these tracts link orbital and medial prefrontal cortical regions to medial temporal regions, with the cingulum functioning as a dorsal limbic pathway, and the uncinate as a ventral limbic pathway (Mori et al., 2005; Schmahmann et al., 2007). The cingulum connects hippocampal regions to the cingulate, with fibers extending to dorsolateral prefrontal cortex (Mori et al., 2005; Schmahmann et al., 2007). The hippocampus and surrounding areas are important for memory function (Mishkin, 1982; Squire and Zola-Morgan, 1991) which have been found to develop past childhood (Ghetti and Bunge, 2012). The dorsolateral prefrontal cortex is involved in working memory and staying on task (Gazzaley and Nobre, 2012; Ikkai and Curtis, 2011) and shows differential activity supporting cognitive performance in development (Luna et al., 2010; Marsh et al., 2008). Further, both these regions show protracted development of synaptic density and myelination (Benes et al., 1994; Huttenlocher and Dabholkar, 1997), supporting their role in the development of cognition through adolescence (Luna et al., 2004). The cingulate cortex is situated between these regions in the circuit. Functional imaging studies demonstrate that the anterior cingulate is involved in both error and reward processing (Walton et al., 2007) and activation associated with these is still immature in adolescence (Eshel et al., 2007; Fjell et al., 2012; Velanova et al., 2008); hence, it may contribute to the development of the link between cognition and emotion through adolescence. This conclusion is supported by our finding of developmental brain-behavior correlation in the cingulum with inhibitory performance.

Whereas the cingulum reached maturation early in the third decade, growth continued throughout our sampled age range in the uncinate fasciculus, late into the third decade. Most of the regions with significant developmental change showed increases in FA and decreases in RD, thus likely related to greater myelination; in contrast, developmental change in the uncinate fasciculus during adulthood was related to increases in FA and increases in AD, more consistent with greater axonal density. Similarly protracted development has been described in the equivalent tract in adolescent rats, specifically related to fiber density (Cunningham et al., 2002). The uncinate fasciculus connects the orbitofrontal cortex to the amygdala and hippocampus, as well as superior and inferior temporal regions (Schmahmann et al., 2007). The orbitofrontal cortex is important for reward processing and decision making (O'Doherty et al., 2003), and is particularly relevant for the development of social behaviors, which show dramatic change in adolescence (Blakemore and Robbins, 2012; Paus et al., 2008). Lesions of the orbitofrontal cortex in adolescent monkeys leads to decreased anxious and fearful behaviors (Kalin et al., 2007) and inability to adjust to social situations (Eslinger et al., 2004). In humans, activation in orbitofrontal cortex is reported in functional imaging studies of social cooperation/competition tasks (Hampton et al., 2008; McCabe et al., 2001) and is associated with risk-taking behaviors (Chein et al., 2011; Shad et al., 2011). The uncinate is also connected to the anterior temporal lobes, which has been shown to play a critical role in representing and retrieving social knowledge (Olson et al., 2012), as well as the amygdala, which is important for emotional development (Tottenham, 2012). Further, connectivity in this tract is abnormal in psychiatric populations; adolescents with disruptive behavioral disorders have decreased functional connectivity between orbitofrontal cortex and amygdala (Marsh et al., 2011), and depressed patients have lower

FA in the uncinate (Versace et al., 2010). Hence, the uncinate is a critical mediator between cognitive and emotional processing, and may be a significant factor in the pathophysiology of adolescent psychopathology.

Consistent with prior studies developmental DTI studies, both AD and RD decreased with development. Furthermore, developmental increases in FA reflect that RD decreases to a greater extent than AD (Wang et al., 2012). RD changes largely mirrored those of FA, suggesting that the majority of the developmental changes in FA are related to myelination (Song et al., 2002; Song et al., 2005). Since AD changes were predominantly decreases, AD increases in the cingulum and uncinate fasciculus during early adulthood are notable and suggest that these limbic changes may be more related to increased axonal density (Cunningham et al., 2002; Song et al., 2002).

This is the first longitudinal DTI study in which a large group of subjects have at least 3 measurements, which is minimum necessary to calculate a statistic on an individual linear trajectory; additional measurements are needed to examine non-linear change. The mixed model regression captures variability both within-person and among individuals, which aids the precision of model estimates and improves the group non-linear fit. Modeling more complex changes within individuals to examine their growth may offer extra insight into individual development; however, we believe that more within-individual measurements are needed to achieve enough sampling through the age range to calculate individual maturation.

In sum, these results suggest a hierarchical maturation of WM where basic sensorimotor and brain stem systems mature first followed by executive systems through adolescence while tracts that support integration of executive and emotion systems continue to mature into adulthood. Prolonged plasticity could provide an adaptive mechanisms for optimal specialization of socio emotional processing during adolescence and early adulthood when social demands change as adult independence is reached (Crone and Dahl, 2012). Prolonged maturation however may also underlie vulnerabilities for abnormal development of socio-emotional processing that may contribute to mood disorders that emerge at this time of development (Paus et al., 2008).

4.2 Sex differences in white matter development

Consistent with previous studies of sex differences in WM development (Asato et al., 2010; De Bellis et al., 2001; Giedd et al., 1999; Wang et al., 2012), males showed larger and more protracted WM microstructural growth, with lower levels of FA than females in childhood and greater levels in adulthood. Due to our non-linear examination of individual growth, we were able to identify that sex differences were concentrated in childhood and adulthood, with growth in males but not in females. Both males and females showed significant growth in WM microstructure during adolescence.

It is possible that sex differences in WM development are driven by differences in pubertal maturation (Lenroot et al., 2007; Peper et al., 2011; Sisk and Foster, 2004), as puberty onset in females occurs 2-3 years earlier than in males (Sisk and Foster, 2004). Developmental DTI studies have shown differences associated with puberty as well as interactions of puberty and sex. These findings show that advancing pubertal maturity is related to

decreases in RD in widespread association and projection tracts (Asato et al., 2010) and increases in FA in insula and frontal white matter (Herting et al., 2012), even after controlling for age. Further, sex hormones were associated with FA, with a positive correlation with testosterone in males, and a negative correlation with estradiol in females (Herting et al., 2012). These findings may provide insight into sex differences in developmental psychopathology, with male-dominant disorders such as attention-deficit/hyperactivity disorder and autism occurring early in development, and female-dominant mood disorders such as anxiety and depression emerging later in adolescence. One potential limitation of findings of sex differences in childhood may be the exclusion of several longitudinal subjects whose data began in childhood during regression diagnostics (see Supplementary Table 1 for these details). However, the majority of the scans during this period were included, and due to the use of splines and the larger sample size for older ages, the remaining data should be very reliable.

4.3 Relation of white matter and behavioral development

Results suggest that differences in the timing of white matter changes may underlie developmental changes in behavior. Consistent with previous studies, we found that RT variability and inhibitory performance continued to mature through adolescence, whereas latency matured earlier (Klein et al., 2005; Luna et al., 2004; Williams et al., 2005). RT variability is a within-individual measure reflecting efficiency of responding to a stimulus; it is correlated with cognitive performance including response inhibition and working memory (Bellgrove et al., 2004; Klein et al., 2006; Simmonds et al., 2007). In our study, RT variability was associated with the timing of white matter development across the whole brain. This finding is consistent with studies showing association of widespread white matter volume and microstructure with RT variability (Tamnes et al., 2012; Walhovd and Fjell, 2007) and suggesting that increases in white matter integrity throughout the brain may facilitate more consistent better network engagement supporting ready access to consistent response execution. Further, we found that earlier WM growth in adolescence was associated with lower RT variability, while later growth in adulthood was associated with greater RT variability. These data results suggest that earlier maturation of white matter may facilitate efficient network integration while individuals with delayed maturation still demonstrate behavioral immaturity reflected in high levels of variability. A similar pattern regarding the timing of white matter development was seen in the left cingulum in relation to the ability to engage cognitive inhibitory control during the AS task. Earlier growth in adolescence was associated with lower error rates, while later growth in adulthood was associated with higher rates, or immature inhibitory control. Regions connected by the cingulum, including dorsolateral prefrontal cortex, cingulate cortex and hippocampus, are critical for cognitive control (Luna et al., 2010). Specifically, fMRI studies have shown that the anterior cingulate cortex and dorsolateral prefrontal cortex has been found to underlie AS performance (Polli et al., 2005) and shows a protracted engagement through adolescence (Eshel et al., 2007; Luna et al., 2010; Velanova et al., 2008). Protracted maturation of the cingulum may contribute to continued improvements in cognitive inhibitory control through adolescence as it supports the ability for the anterior cingulate to integrate with other regions of the brain to affect behavior (Klein et al., 2005; Luna et al., 2004).

4.4 Conclusion

The present study characterized the timing and stages of WM development. In contrast with the majority of brain developmental studies characterizing development as a continuous process, this study examines growth in discrete stages, which is how much of biological development proceeds. We found that for some regions, WM growth slowed in adolescence before speeding up in early adulthood. Further, understanding the timing of brain development and how it relates to individual differences in biology and behavior is critical for understanding the many neurological and psychiatric diseases that emerge throughout adolescence. These diseases emerge at different times, in different sexes and with different behavioral manifestations, which may be due to differences in within-individual change. Hence, understanding within-individual growth patterns over development is necessary before identifying and interpreting differences in clinical developmental populations. Taken together, these results suggest that WM maturation matures in a hierarchical manner with pathways that support executive control maturing through adolescence while those supporting socio-emotional processing continuing through the twenties. Males show later maturation than females perhaps underlying vulnerabilities to psychiatric disorders that emerge in childhood vs. adolescence. Evidence that continued WM growth during adolescence supports better cognitive performance while delayed maturation into adulthood underlies worse performance suggests that cognitive outcomes are influenced by the timing of specific neurodevelopmental processes, which may also help explain psychiatric vulnerability during this time.

Supplementary Material

Refer to Web version on PubMed Central for supplementary material.

References

Armstrong E, Schleicher A, Omran H, Curtis M, Zilles K. The ontogeny of human gyrification. Cereb. Cortex. 1995; 5:56–63. [PubMed: 7719130]

Asato MR, Terwilliger R, Woo J, Luna B. White Matter Development in Adolescents: A DTI Study. Cereb. Cortex. 2010; 20:2122–2131. [PubMed: 20051363]

Barnea-Goraly N, Menon V, Eckert M, Tamm L, Bammer R, Karchemskiy A, Dant CC, Reiss AL. White matter development during childhood and adolescence: a cross-sectional diffusion tensor imaging study. Cereb. Cortex. 2005; 15:1848–1854. [PubMed: 15758200]

Bava S, Thayer R, Jacobus J, Ward M, Jernigan TL, Tapert SF. Longitudinal characterization of white matter maturation during adolescence. Brain Res. 2010; 1327:38–46. [PubMed: 20206151]

Bedard AC, Nichols S, Barbosa JA, Schachar R, Logan GD, Tannock R. The development of selective inhibitory control across the life span. Dev. Neuropsychol. 2002; 21:93–111. [PubMed: 12058837]

Bellgrove, M. a; Hester, R.; Garavan, H. The functional neuroanatomical correlates of response variability: evidence from a response inhibition task. Neuropsychologia. 2004; 42:1910–6. [PubMed: 15381021]

Benes FM, Turtle M, Khan Y, Farol P. Myelination of a key relay zone in the hippocampal formation occurs in the human brain during childhood, adolescence, and adulthood. Arch. Gen. Psychiatry. 1994; 51:477–484. [PubMed: 8192550]

Blakemore S-J, Robbins TW. Decision-making in the adolescent brain. Nat. Neurosci. 2012; 15:1184–1191. [PubMed: 22929913]

Burchinal M, Appelbaum MI. Estimating Individual Developmental Functions: Methods and Their Assumptions. Child Dev. 1991; 62:23–43.

Casey BJ, Durston S. From behavior to cognition to the brain and back: what have we learned from functional imaging studies of attention deficit hyperactivity disorder? Am. J. Psychiatry. 2006; 163:957–960. [PubMed: 16741192]

Chein J, Albert D, O'Brien L, Uckert K, Steinberg L. Peers increase adolescent risk taking by enhancing activity in the brain's reward circuitry. Dev. Sci. 2011; 14:F1–F10. [PubMed: 21499511]

Cook, RD.; Weisberg, S. Residuals and influence in regression. Chapman and Hall; 1982.

Crone EA, Dahl RE. Understanding adolescence as a period of social–affective engagement and goal flexibility. Nat. Rev. Neurosci. 2012; 13:636–650. [PubMed: 22903221]

Cunningham MG, Bhattacharyya S, Benes FM. Amygdalo-cortical sprouting continues into early adulthood: Implications for the development of normal and abnormal function during adolescence. J. Comp. Neurol. 2002; 453:116–130. [PubMed: 12373778]

De Bellis MD, Keshavan MS, Beers SR, Hall J, Frustaci K, Masalehdan A, Noll J, Boring AM. Sex Differences in Brain Maturation during Childhood and Adolescence. Cereb. Cortex. 2001; 11:552–557. [PubMed: 11375916]

Dosenbach NUF, Fair DA, Miezin FM, Cohen AL, Wenger KK, Dosenbach RAT, Fox MD, Snyder AZ, Vincent JL, Raichle ME, Schlaggar BL, Petersen SE. Distinct brain networks for adaptive and stable task control in humans. Proc. Natl. Acad. Sci. 2007; 104:11073–11078. [PubMed: 17576922]

Dosenbach NU, Nardos B, Cohen AL, Fair DA, Power JD, Church JA, Nelson SM, Wig GS, Vogel AC, Lessov-Schlaggar CN, Barnes KA, Dubis JW, Feczko E, Coalson RS, Pruett JR Jr, Barch DM, Petersen SE, Schlaggar BL. Prediction of individual brain maturity using fMRI. Science. 2010; 329(5997):1358–1361. [PubMed: 20829489]

Eshel N, Nelson EE, Blair RJ, Pine DS, Ernst M. Neural substrates of choice selection in adults and adolescents: Development of the ventrolateral prefrontal and anterior cingulate cortices. Neuropsychologia. 2007; 45:1270–1279. [PubMed: 17118409]

Eslinger PJ, Flaherty-Craig CV, Benton AL. Developmental outcomes after early prefrontal cortex damage. Brain Cogn. 2004; 55:84–103. [PubMed: 15134845]

Filipek PA, Richelme C, Kennedy DN, Caviness VS. The young adult human brain: an MRI-based morphometric analysis. Cereb. Cortex. 1994; 267:344–360. [PubMed: 7950308]

Fischer B, Gezeck S, Hartnegg K. The analysis of saccadic eye movements from gap and overlap paradigms. Brain Res. Protoc. 1997; 2:47–52.

Fjell AM, Walhovd KB, Brown TT, Kuperman JM, Chung Y, et al. Multimodal imaging of the self-regulating developing brain. Proc. Natl. Acad. Sci. 2012; 109:19620–19625. [PubMed: 23150548]

Fukushima J, Hatta T, Fukushima K. Development of voluntary control of saccadic eye movements. I. Age-related changes in normal children. Brain Dev. 2000; 22:173–180. [PubMed: 10814900]

Gazzaley A, Nobre AC. Top-down modulation: bridging selective attention and working memory. Trends Cogn. Sci. 2012; 16:129–135. [PubMed: 22209601]

Ghetti S, Bunge SA. Neural changes underlying the development of episodic memory during middle childhood. Dev. Cogn. Neurosci. 2012; 2:381–395. [PubMed: 22770728]

Giedd JN, Blumenthal J, Jeffries NO, Castellanos FX, Liu H, Zijdenbos A, Paus T, Evans AC, Rapoport JL. Brain development during childhood and adolescence: a longitudinal MRI study. Nat Neurosci. 1999; 2:861–3. [PubMed: 10491603]

Giorgio A, Watkins KE, Chadwick M, James S, Winmill L, Douaud G, De Stefano N, Matthews PM, Smith SM, Johansen-Berg H, James AC. Longitudinal changes in grey and white matter during adolescence. NeuroImage. 2009; 49:94–103. [PubMed: 19679191]

Giorgio A, Watkins KE, Douaud G, James AC, James S, De Stefano N, Matthews PM, Smith SM, Johansen-Berg H. Changes in white matter microstructure during adolescence. NeuroImage. 2008; 39:52–61. [PubMed: 17919933]

Gong G, Jiang T, Zhu C, Zang Y, He Y, Xie S, Xiao J. Side and handedness effects on the cingulum from diffusion tensor imaging. Neuroreport. 2005; 16(15):1701–1705. [PubMed: 16189481]

Hallett PE. Primary and secondary saccades to goals defined by instructions. Vision Res. 1978; 18:1279–1296. [PubMed: 726270]

Hampton AN, Bossaerts P, O'Doherty JP. Neural correlates of mentalizing-related computations during strategic interactions in humans. Proc. Natl. Acad. Sci. 2008; 105:6741–6746. [PubMed: 18427116]

Hermoye L, Saint-Martin C, Cosnard G, Lee S-K, Kim J, Nassogne M-C, Menten R, Clapuyt P, Donohue PK, Hua K, Wakana S, Jiang H, van Zijl PCM, Mori S. Pediatric diffusion tensor imaging: Normal database and observation of the white matter maturation in early childhood. NeuroImage. 2006; 29:493–504. [PubMed: 16194615]

Herting MM, Maxwell EC, Irvine C, Nagel BJ. The impact of sex, puberty and hormones on white matter microstructure in adolescents. Cereb. Cortex. 2012; 22(9):1979–1992. [PubMed: 22002939]

Holm S. A Simple Sequentially Rejective Multiple Test Procedure. Scand. J. Stat. 1979; 6:65–70.

Huttenlocher PR. Morphometric study of human cerebral cortex development. Neuropsychologia. 1990; 28:517–27. [PubMed: 2203993]

Huttenlocher PR, Dabholkar AS. Regional differences in synaptogenesis in human cerebral cortex. J. Comp. Neurol. 1997; 387:167–178. [PubMed: 9336221]

Ikkai A, Curtis CE. Common neural mechanisms supporting spatial working memory, attention and motor intention. Neuropsychologia. 2011; 49:1428–1434. [PubMed: 21182852]

Kail R. Processing time decreases globally at an exponential rate during childhood and adolescence. J. Exp. Child Psychol. 1993; 56:254–265. [PubMed: 8245769]

Kalin NH, Shelton SE, Davidson RJ. Role of the Primate Orbitofrontal Cortex in Mediating Anxious Temperament. Biol. Psychiatry. 2007; 62:1134–1139. [PubMed: 17643397]

Klein C, Foerster F. Development of prosaccade and antisaccade task performance in participants aged 6 to 26 years. Psychophysiology. 2001; 38:179–189. [PubMed: 11347863]

Klein C, Foerster F, Hartnegg K, Fischer B. Lifespan development of pro- and anti-saccades: multiple regression models for point estimates. Dev. Brain Res. 2005; 160:113–123. [PubMed: 16266754]

Klein C, Wendling K, Huettner P, Ruder H, Peper M. Intra-subject variability in attention-deficit hyperactivity disorder. Biol. Psychiatry. 2006; 60:1088–97. [PubMed: 16806097]

Lebel C, Beaulieu C. Longitudinal Development of Human Brain Wiring Continues from Childhood into Adulthood. J. Neurosci. 2011; 31:10937–10947. [PubMed: 21795544]

Lebel C, Gee M, Camicioli R, Wieler M, Martin W, Beaulieu C. Diffusion tensor imaging of white matter tract evolution over the lifespan. Neuroimage. 2012; 60:340–352. [PubMed: 22178809]

Lebel C, Walker L, Leemans a, Phillips L, Beaulieu C. Microstructural maturation of the human brain from childhood to adulthood. NeuroImage. 2008; 40:1044–55. [PubMed: 18295509]

Lenroot RK, Gogtay N, Greenstein DK, Wells EM, Wallace GL, Clasen LS, Blumenthal JD, Lerch J, Zijdenbos AP, Evans AC, Thompson PM, Giedd JN. Sexual dimorphism of brain developmental trajectories during childhood and adolescence. NeuroImage. 2007; 36:1065–1073. [PubMed: 17513132]

Liston C, Watts R, Tottenham N, Davidson MC, Niogi S, Ulug AM, Casey BJ. Frontostriatal Microstructure Modulates Efficient Recruitment of Cognitive Control. Cereb. Cortex. 2006; 16:553–560. [PubMed: 16033925]

Liu Z, Wang Y, Gerig G, Gouttard S, Tao R, Fletcher T, Styner M. Quality control of diffusion weighted images. Changes. 2010; 1:76280J–76280J–9.

Luna, B. Methodological and Clinical Trends. Springer-Verlag; Berlin Heidelberg: 2009. The Maturation of Cognitive Control and the Adolescent Brain, in: From Attention to Goal-Directed Behavior: Neurodynamical; p. 249-274.

Luna B, Garver KE, Urban TA, Lazar NA, Sweeney JA. Maturation of cognitive processes from late childhood to adulthood. Child Dev. 2004; 75:1357–1372. [PubMed: 15369519]

Luna B, Padmanabhan A, O'Hearn K. What has fMRI told us about the development of cognitive control through adolescence? Brain Cogn. 2010; 72:101–13. [PubMed: 19765880]

Marsh AA, Finger EC, Fowler KA, Jurkowitz ITN, Schechter JC, Yu HH, Pine DS, Blair RJR. Reduced amygdala–orbitofrontal connectivity during moral judgments in youths with disruptive behavior disorders and psychopathic traits. Psychiatry Res. Neuroimaging. 2011; 194:279–286.

Marsh R, Gerber AJ, Peterson BS. Neuroimaging studies of normal brain development and their relevance for understanding childhood neuropsychiatric disorders. J. Am. Acad. Child Adolesc. Psychiatry. 2008; 47:1233–51. [PubMed: 18833009]

McCabe K, Houser D, Ryan L, Smith V, Trouard T. A functional imaging study of cooperation in two-person reciprocal exchange. Proc. Natl. Acad. Sci. 2001; 98:11832–11835. [PubMed: 11562505]

Middleton FA, Strick PL. Basal ganglia output and cognition: evidence from anatomical, behavioral, and clinical studies. Brain Cogn. 2000; 42:183–200. [PubMed: 10744919]

Mishkin M. A memory system in the monkey. Philos. Trans. R. Soc. Lond. B. Biol. Sci. 1982; 298:83–95. [PubMed: 6125978]

Mori, S.; Wakana, S.; van Zijl, PCM.; Nagae-Poetscher, LM. MRI Atlas of Human White Matter. Elsevier B. V.; Amsterdam: 2005.

Mukherjee P, Miller JH, Shimony JS, Conturo TE, Lee BCP, Almli CR, McKinstry RC. Normal brain maturation during childhood: Developmental trrends characterized with diffusion-tensor MR imaging. Radiology. 2001; 221:349–358. [PubMed: 11687675]

Munoz DP, Broughton JR, Goldring JE, Armstrong IT. Age-related performance of human subjects on saccadic eye movement tasks. Exp. Brain Res. 1998; 121:391–400. [PubMed: 9746145]

Nagy Z, Westerberg H, Klingberg T. Maturation of white matter is associated with the development of cognitive functions during childhood. J Cogn Neurosci. 2004; 16:1227–1233. [PubMed: 15453975]

O'Doherty J, Critchley H, Deichmann R, Dolan RJ. Dissociating valence of outcome from behavioral control in human orbital and ventral prefrontal cortices. J. Neurosci. Off. J. Soc. Neurosci. 2003; 23:7931–9.

Olson IR, McCoy D, Klobusicky E, Ross LA. Social Cognition and the Anterior Temporal Lobes: A Review and Theoretical Framework. Soc. Cogn. Affect. Neurosci. 2012

Paus T, Keshavan M, Giedd JN. Why do many psychiatric disorders emerge during adolescence? Nat. Rev. Neurosci. 2008; 9:947–957. [PubMed: 19002191]

Peper JS, Pol HEH, Crone E. a, van Honk J. Sex steroids and brain structure in pubertal boys and girls: a mini-review of neuroimaging studies. Neuroscience. 2011

Petanjek Z, Judaš M, Šimić G, Rašin MR, Uylings HBM, Rakic P, Kostović I. Extraordinary neoteny of synaptic spines in the human prefrontal cortex. Proc. Natl. Acad. Sci. 2011; 108:13281–13286. [PubMed: 21788513]

Pfefferbaum A, Mathalon DH, Sullivan EV, Rawles JM, Zipursky RB, Lim KO. A quantitative magnetic resonance imaging study of changes in brain morphology from infancy to late adulthood. Arch. Neurol. 1994; 51:874–887. [PubMed: 8080387]

Pinheiro, JC.; Bates, DM. Mixed-Effects Models in S, S-PLUS. Springer; New York: 2000.

Polli FE, Barton JJ, Cain MS, Thakkar KN, Rauch SL, Manoach DS. Rostral and dorsal anterior cingulate cortex make dissociable contributions during antisaccade error commission. Proc. Natl. Acad. Sci. U. S. A. 2005; 102:15700–15705. [PubMed: 16227444]

R Core Team. R: A Language and Environment for Statistical Computing. 2012

Reiss AL, Abrams MT, Singer HS, Ross JL, Denckla MB. Brain development, gender and IQ in children A volumetric imaging study. Brain. 1996; 119:1763–1774. [PubMed: 8931596]

Rogosa D, Brandt D, Zimowski M. A growth curve approach to the measurement of change. Psychol. Bull. 1982; 92:726–748.

Sauseng P, Klimesch W, Schabus M, Doppelmayr M. Fronto-parietal EEG coherence in theta and upper alpha reflect central executive functions of working memory. Int. J. Psychophysiol. 2005; 57:97–103. [PubMed: 15967528]

Schmahmann, JD.; Pandya, DN. Fiber pathways of the brain. Oxford University Press; NY.: 2006.

Schmahmann JD, Pandya DN, Wang R, Dai G, D'Arceuil HE, Crespigny AJ, de, Wedeen VJ. Association fibre pathways of the brain: parallel observations from diffusion spectrum imaging and autoradiography. Brain. 2007; 130:630–653. [PubMed: 17293361]

Schmithorst VJ, Wilke M, Dardzinski BJ, Holland SK. Correlation of white matter diffusivity and anisotropy with age during childhood and adolescence: a cross-sectional diffusion-tensor MR imaging study. Radiology. 2002; 222:212–218. [PubMed: 11756728]

Shad MU, Bidesi AS, Chen L-A, Thomas BP, Ernst M, Rao U. Neurobiology of decision-making in adolescents. Behav. Brain Res. 2011; 217:67–76. [PubMed: 20933020]

Simmonds DJ, Fotedar SG, Suskauer SJ, Pekar JJ, Denckla MB, Mostofsky SH. Functional brain correlates of response time variability in children. Neuropsychologia. 2007; 45:2147–57. [PubMed: 17350054]

Singer, JD.; Willett, JB. Applied Longitudinal Data Analysis: Modeling change and event occurrence. Oxford University Press; New York: 2003.

Sisk CL, Foster DL. The neural basis of puberty and adolescence. Nat. Neurosci. 2004; 7:1040–7. [PubMed: 15452575]

Smith SM, Jenkinson M, Johansen-Berg H, Rueckert D, Nichols TE, Mackay CE, Watkins KE, Ciccarelli O, Cader MZ, Matthews PM, Behrens TEJ. Tract-based spatial statistics: voxelwise analysis of multi-subject diffusion data. NeuroImage. 2006; 31:1487–505. [PubMed: 16624579]

Smith SM, Jenkinson M, Woolrich MW, Beckmann CF, Behrens TEJ, Johansen-Berg H, Bannister PR, De Luca M, Drobnjak I, Flitney DE, Niazy RK, Saunders J, Vickers J, Zhang Y, De Stefano N, Brady JM, Matthews PM. Advances in functional and structural MR image analysis and implementation as FSL. NeuroImage. 2004; 23(Supplement 1):S208–S219. [PubMed: 15501092]

Song SK, Sun SW, Ramsbottom MJ, Chang C, Russell J, Cross AH. Dysmyelination revealed through MRI as increased radial (but unchanged axial) diffusion of water. NeuroImage. 2002; 17:1429–-1436. [PubMed: 12414282]

Song SK, Yoshino J, Le TQ, Lin SJ, Sun SW, Cross AH, Armstrong RC. Demyelination increases radial diffusivity in corpus callosum of mouse brain. NeuroImage. 2005; 26:132–-140. [PubMed: 15862213]

Spear LP. The adolescent brain and age-related behavioral manifestations. Neurosci.Biobehav.Rev. 2000; 24:417–463. [PubMed: 10817843]

Squire LR, Zola-Morgan S. The medial temporal lobe memory system. Science. 1991; 253:1380–1386. [PubMed: 1896849]

Tamnes CK, Fjell a. M. Westlye LT, Ostby Y, Walhovd KB. Becoming Consistent: Developmental Reductions in Intraindividual Variability in Reaction Time Are Related to White Matter Integrity. J. Neurosci. 2012; 32:972–982. [PubMed: 22262895]

Tamnes CK, Ostby Y, Fjell AM, Westlye LT, Due-Tø nnessen P, Walhovd KB. Brain maturation in adolescence and young adulthood: regional age-related changes in cortical thickness and white matter volume and microstructure. Cereb. Cortex New York N 1991. 2010; 20:534–48.

Thatcher RW. Cyclic cortical reorganization during early childhood. Brain Cogn. 1992; 20:24–50. [PubMed: 1389121]

Tottenham N. Human amygdala development in the absence of species-expected caregiving. Dev. Psychobiol. 2012; 54:598–611. [PubMed: 22714586]

Velanova K, Wheeler ME, Luna B. Maturational Changes in Anterior Cingulate and Frontoparietal Recruitment Support the Development of Error Processing and Inhibitory Control. Cereb. Cortex. 2008; 18:2505–2522. [PubMed: 18281300]

Versace A, Almeida JRC, Quevedo K, Thompson WK, Terwilliger RA, Hassel S, Kupfer DJ, Phillips ML. Right Orbitofrontal Corticolimbic and Left Corticocortical White Matter Connectivity Differentiate Bipolar and Unipolar Depression. Biol. Psychiatry. 2010; 68:560–567. [PubMed: 20598288]

Vestergaard M, Madsen KS, Baaré WFC, Skimminge A, Ejersbo LR, Ramsøy TZ, Gerlach C, Akeson P, Paulson OB, Jernigan TL. White matter microstructure in superior longitudinal fasciculus associated with spatial working memory performance in children. J. Cogn. Neurosci. 2011; 23:2135–2146. [PubMed: 20964591]

Vincent JL, Kahn I, Snyder AZ, Raichle ME, Buckner RL. Evidence for a Frontoparietal Control System Revealed by Intrinsic Functional Connectivity. J. Neurophysiol. 2008; 100:3328–3342. [PubMed: 18799601]

Wahl M, Li Y-O, Ng J, Lahue SC, Cooper SR, Sherr EH, Mukherjee P. Microstructural correlations of white matter tracts in the human brain. NeuroImage. 2010; 51:531–41. [PubMed: 20206699]

Walhovd KB, Fjell AM. White matter volume predicts reaction time instability. Neuropsychologia. 2007; 45:2277–84. [PubMed: 17428508]

Walton ME, Croxson PL, Behrens TEJ, Kennerley SW, Rushworth MFS. Adaptive decision making and value in the anterior cingulate cortex. NeuroImage. 2007; 36(Supplement 2):T142–T154. [PubMed: 17499161]

Wang Y, Adamson C, Yuan W, Altaye M, Rajagopal A, Byars AW, Holland SK. Sex differences in white matter development during adolescence: A DTI study. Brain Res. 2012; 1478:1–15. [PubMed: 22954903]

Wechsler, D. WAIS-R Wechsler adult intelligence scale-revised. The Psychological Corporation; New York: 1981.

Wickham, H. ggplot2: elegant graphics for data analysis. Springer; New York: 2009.

Williams BR, Hultsch DF, Strauss EH, Hunter MA, Tannock R. Inconsistency in reaction time across the life span. Neuropsychology. 2005; 19:88–96. [PubMed: 15656766]

Williams BR, Ponesse JS, Schachar RJ, Logan GD, Tannock R. Development of inhibitory control across the life span. Dev. Psychol. 1999; 35:205–13. [PubMed: 9923475]

Yakovlev, PI.; Lecours, AR. Regional Development of the Brain in Early Life. Blackwell Scientific; Oxford: 1967. The myelogenetic cycles of regional maturation of the brain; p. 3-70.

Highlights

- We find hierarchical white matter (WM) development in a longitudinal sample
- Maturation of most frontal connectivity in adolescence supports cognitive function
- Late maturation of corticolimbic connectivity supports socioemotional interactions
- Males showed WM growth from childhood to adulthood, females mainly in mid-adolescence
- Delayed maturation of WM was associated with poorer cognitive performance

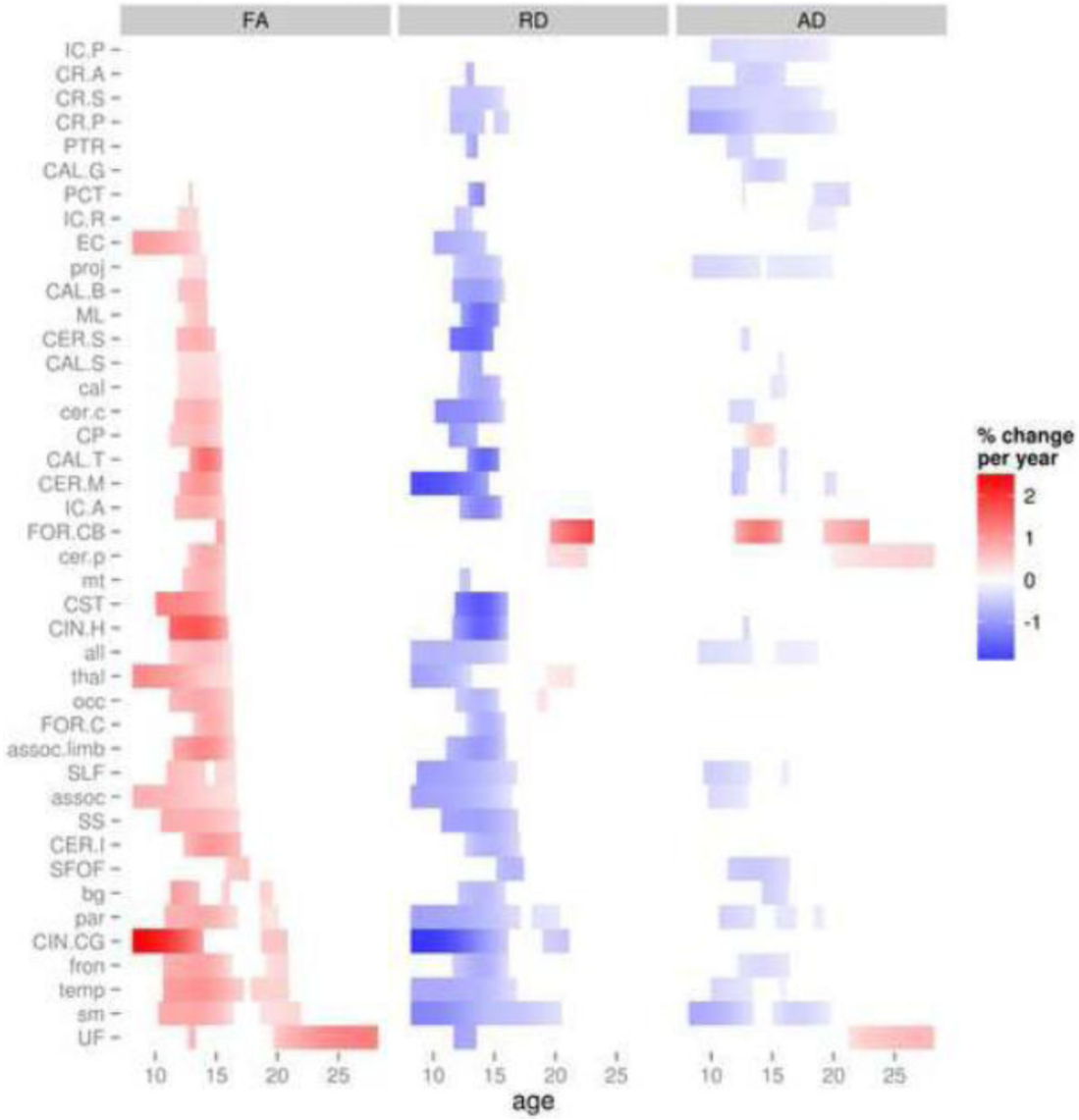

Figure 1. Stages of significant growth and timing of maturation in white matter development

Figure is divided into three columns corresponding to FA, RD and AD, respectively. Developmental changes in FA were all increases, while those in RD and AD were mostly decreases. Each row is an ROI whose label abbreviation is explained in Table 1; rows are sorted by time of maturation in FA, which is defined as the time that the rate of change was no longer significantly different from the null (p=0.05, bootstrap corrected). Colors represent % change per year (red=increase, blue=decrease).

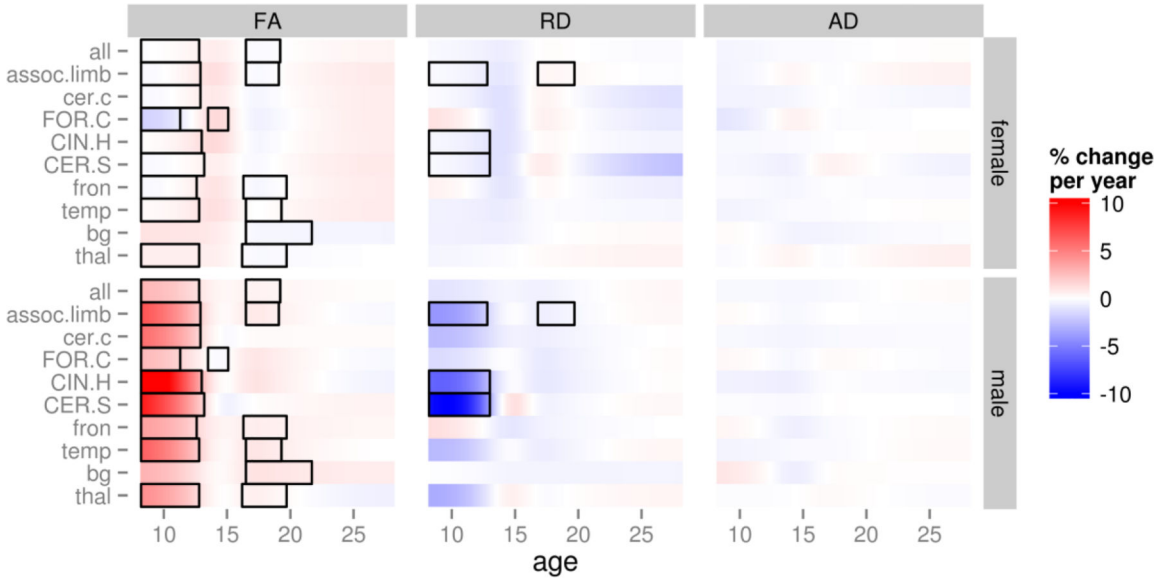

Figure 2. Sex differences in white matter development

Figure is divided into three columns corresponding to FA, RD and AD, respectively; it is further divided by sex (top=female, bottom=male). Differences were predominantly seen during childhood and late adolescence/early adulthood, representing greater change of FA and RD in males (no significant differences were seen for AD). Each row is an ROI whose label abbreviation is explained in Table 1; ROIs shown in the figure were significant for at least one of the three measures. Colors represent % change per year (red=increase, blue=decrease). Black rectangles indicate stages with significant sex differences.

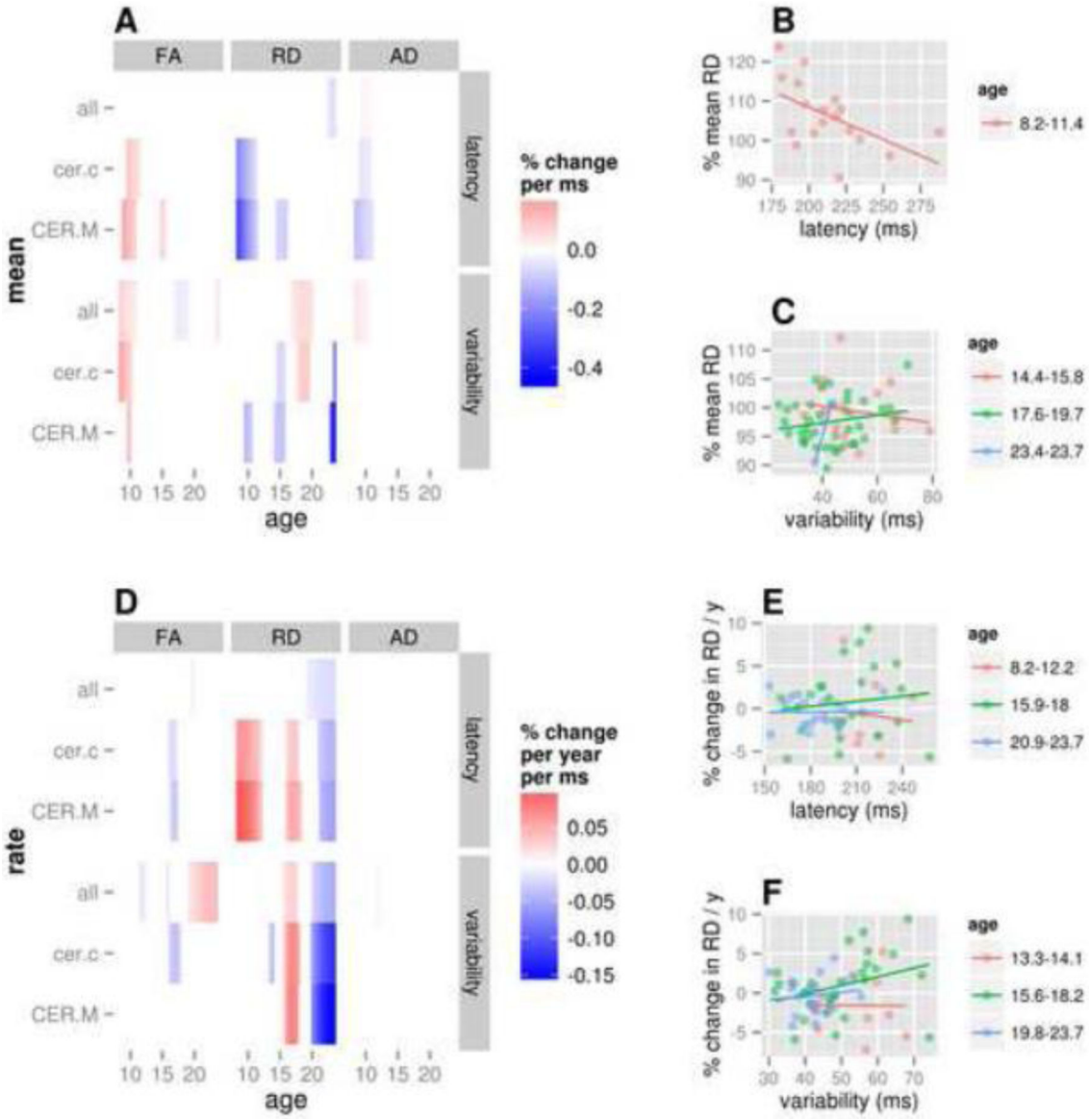

Figure 3. Associations between VGS latency/variability and WM development

Heatmaps represent the association between the behavioral variables and (A) mean WM levels and (D) rates of change in WM development. These plots are divided into three columns corresponding to FA, RD and AD, respectively; they are further divided by behavioral variable (top=latency, bottom=variability). Each row is an ROI whose label abbreviation is explained in Table 1; included ROIs were significant for at least one of the three measures. RD was the only measure significantly associated with latency, while FA and RD were both related to variability. Colors represent magnitude of brain behavior correlation (red=positive, blue=negative). The scatterplots further illustrate these associations in a single region (cer.c) for the measure RD by showing individual subject brain and behavioral measures within significant stages of association; data points (single scans or scan-to-scan changes) were included if they fell within the stage (in some cases, subjects have multiple points plotted). For each stage, a simple linear fit is shown

highlighting the direction of association (B: mean-level RD vs. latency; C: mean-level RD vs. variability; E: rate of change in RD vs. latency; F: rate of change in RD vs. variability). Colors in these plots represent different significant stages of association, with ages identified in the legends.

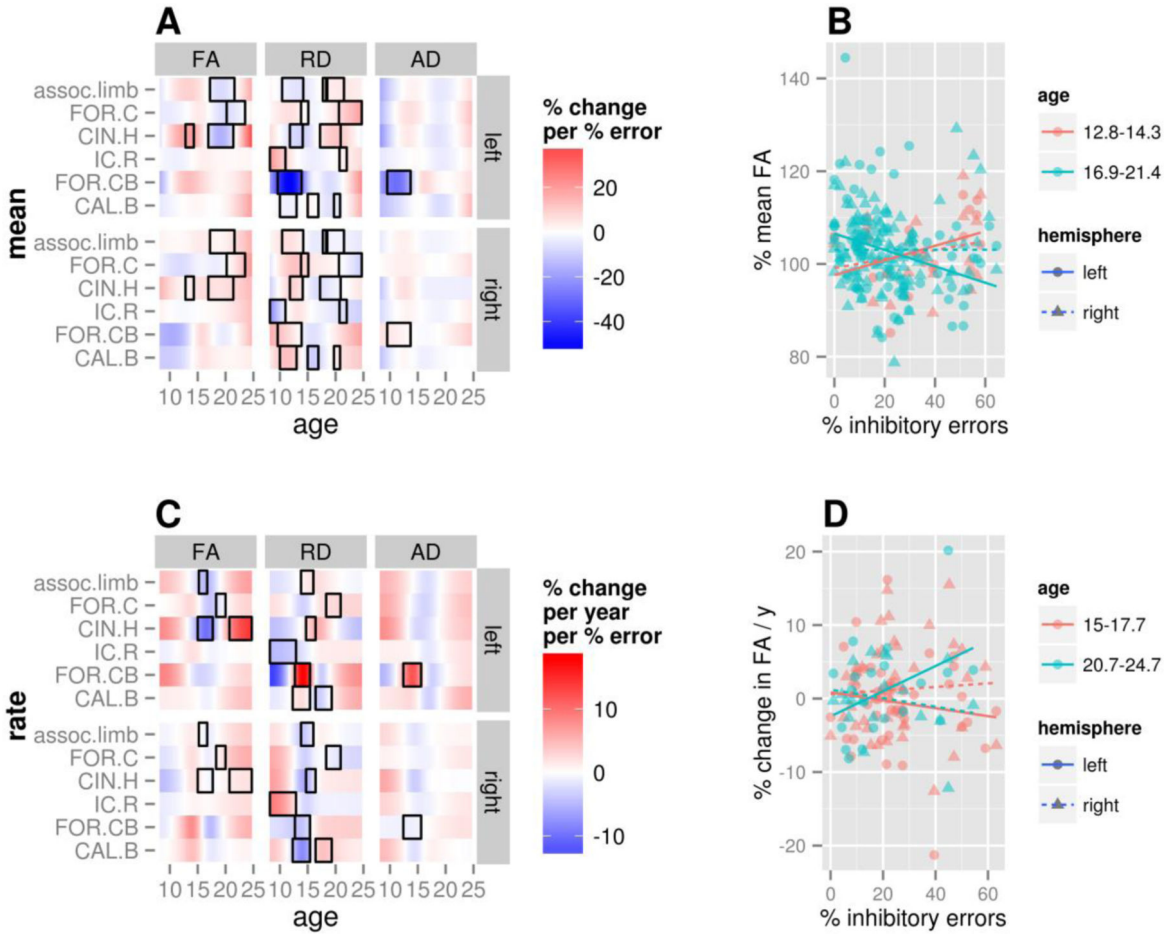

Figure 4. Associations between inhibitory errors, white matter development and hemispheric differences

Heatmaps represent the association between behavior and (A) mean WM levels and (C) rates of change in WM development. These plots are divided into three columns corresponding to FA, RD and AD, respectively; they are further divided by hemisphere (top=left, bottom=right). Each row is an ROI whose label abbreviation is explained in Table 1; included ROIs were significant for at least one of the three measures. Colors represent magnitude of brain behavior correlation (red=positive, blue=negative). Black rectangles indicate stages with significant hemispheric differences in brain-behavior associations. These differences predominantly reflect significant brain-behavior correlations in the left hemisphere, but not the right. The scatterplots further illustrate these associations in a single region (CIN.H) for the measure FA by showing individual subject brain and behavioral measures within significant stages of association; data points (single scans or scan-to-scan changes) were included if they fell within the stage (in some cases, subjects have multiple points plotted). For each stage, a simple linear fit highlighting the direction of association (B: mean-level FA vs. inhibitory errors; D: rate of change in FA vs. inhibitory errors). Colors in these plots represent different significant stages of association, with ages identified in the legends. Hemispheres are plotted separately (left=circles/solid line, right=triangles/dotted line).

Table 1

Description of ROIs included in analysis.

group	name	connection	abbreviation
	all WM average	all	all
core tract groups	projection	cortical <> subcortical	proj
	association	cortical <> cortical	assoc
	limbic	cortical <> limbic	assoc.limb
	callosal	interhemispheric	cal
	cerebellar	cerebellar input/output	cer.c
projection tracts	medial lemniscus	spinal cord <> brainstem	ML
	pontine crossing tract	spinal cord and cerebellar crossing fibers	PCT
	corticospinal tract (brainstem portion)	sensorimotor	CST
	cerebral peduncle	brainstem <> internal capsule	CP
	internal capsule (anterior)	thalamus <> frontal cortical	IC.A
	internal capsule (posterior)	corticospinal and thalamocortical	IC.P
	internal capsule (retrolenticular)	thalamus <> posterior cortical	IC.R
	corona radiata (anterior)	internal capsule <> cortical	CR.A
	corona radiata (superior)	internal capsule <> cortical	CR.S
	corona radiata (posterior)	internal capsule <> cortical	CR.P
	posterior thalamic radiation	optic radiation	PTR
association tracts	superior fronto-occipital fasciculus	frontal <> parietal <> occipital	SFOF
	sagittal stratum	frontal <> occipital <> temporal	SS
	external capsule	frontal <> parietal <> occipital <> temporal	EC
	uncinate fasciculus	hippocampus <> orbitofrontal cortex	UF
	superior longitudinal fasciculus	frontal <> parietal <> occipital <> temporal	SLF
limbic tracts	fornix (column/body)	hippocampus <> septal nuclei	FOR.CB
	fornix (crescent)	hippocampus <> septal nuclei	FOR.C
	cingulum (cingulate portion)	hippocampus <> parietal <> frontal	CIN.CG
	cingulum (hippocampal portion)	hippocampus <> parietal <> frontal	CIN.H
callosal tracts	corpus callosum (genu)	interhemispheric frontal	CAL.G
	corpus callosum (body)	interhemispheric sensorimotor/posterior	CAL.B
	corpus callosum (splenium)	interhemispheric posterior	CAL.S

group	name	connection	abbreviation
	corpus callosum (tapetum)	interhemispheric posterior	CAL.T
cerebellar tracts	cerebellar peduncle (inferior)	cerebellar input	CER.I
	cerebellar peduncle (middle)	cerebellar input	CER.M
	cerebellar peduncle (superior)	cerebellar output	CER.S
cortical RTZs	parietal		par
	occipital		occ
	sensorimotor		sm
	frontal		fron
	temporal		temp
subcortical RTZs	cerebellar		cer.p
	medial temporal		mt
	basal ganglia		bg
	thalamus		thal

A description of the ROI and abbreviations used in figures and tables are detailed as well. Shading is used as a visual aid to separate groups of ROIs, identifying separate groups used for Holm corrections (see section 2.3 for more details).

Neuroimage. Author manuscript; available in PMC 2015 May 15.

Table 2

WM developmental timing and stages in all included regions for FA.

name	age range (age of peak growth)	FA range (% change/year)	p
all	11.2-16.3 (13.7)	0.442-0.454 (0.529)	5.5e-06 *
proj	12.3-14.2 (13.7)	0.572-0.576 (0.291)	0.14
assoc	8.2-16.7 (8.2)	0.472-0.495 (0.565)	4.4e-07 *
assoc.limb	11.5-16.5 (13.9)	0.47-0.492 (0.923)	5.1e-09 *
cal	11.9-15.4 (13.7)	0.655-0.664 (0.377)	0.0062 *
cer.c	11.6-15.5 (13.6)	0.533-0.547 (0.644)	0.00046 *
ML	12.4-14.3 (13.8)	0.668-0.674 (0.484)	0.15
PCT	12.8-13 (13)	0.51-0.511 (0.377)	0.38
CST	10.1-15.8 (10.1)	0.551-0.583 (1.03)	7.1e-07 #
CP	11.2-15.5 (13.6)	0.674-0.691 (0.557)	3.9e-05 #
IC.A	11.6-15.7 (13.6)	0.579-0.596 (0.677)	7.6e-05 #
IC.P			0.65
IC.R	11.9-13.5 (11.9)	0.582-0.586 (0.382)	0.03
CR.A			0.73
CR.S			0.26
CR.P			0.69
PTR			0.31
SFOF	15.8-17.7 (17)	0.55-0.556 (0.511)	0.17
SS	10.5-16.9 (10.5)	0.53-0.554 (0.677)	1.2e-07 *#
EC	8.2-13.7 (8.2)	0.452-0.471 (0.765)	7e-04 *#
UF	12.7-13.3; 19.7-28.2 (13.3; 28.2)	0.513-0.515; 0.526-0.572 (0.0426; 0.954)	0.0064 *
SLF	11-14.1; 14.9-16.6 (11; 14.9)	0.472-0.48; 0.482-0.485 (0.36; 0.126)	0.00024 *#
FOR.CB	15-15.7 (15)	0.482-0.485 (0.752)	0.16
FOR.C	13.1-16.4 (14.6)	0.508-0.519 (0.638)	0.0018 *#
CIN.CG	8.2-13.9; 18.7-20.8 (8.2; 20.8)	0.459-0.512; 0.527-0.533 (1.43; 0.146)	3.3e-07 *#
CIN.H	11.2-16 (13.5)	0.415-0.444 (1.45)	1.7e-06 *#

name	age range (age of peak growth)	FA range (% change/year)	p
CAL.G			0.74
CAL.B	11.9-14.2 (13.4)	0.581-0.589 (0.566)	0.02
CAL.S	11.9-15.3 (13.5)	0.709-0.717 (0.329)	0.0035 *
CAL.T	12.8-15.5 (14.2)	0.526-0.544 (1.17)	0.022
CER.I	12.4-17 (14.5)	0.414-0.431 (0.853)	0.00013 *#
CER.M	12-15.5 (13.8)	0.526-0.542 (0.873)	0.0039 *
CER.S	11.8-14.9 (13.5)	0.617-0.63 (0.685)	0.0014 *#
par	10.8-16.7; 18.6-20.1 (13.5; 20.1)	0.379-0.395; 0.397-0.399 (0.554; 0.0548)	9.7e-10 *
occ	11.2-16.4 (13.7)	0.369-0.383 (0.71)	9.3e-08 *
sm	10.3-16.4; 18.6-21.9 (13.3; 21.9)	0.406-0.425; 0.427-0.432 (0.482; 0.118)	4.9e-11 *
fron	10.7-16.3; 19.1-20.9 (13.5; 20.9)	0.373-0.389; 0.392-0.395 (0.568; 0.084)	4e-09 *
temp	10.7-17.2; 17.9-20.9 (13.6; 20.9)	0.334-0.353; 0.354-0.359 (0.6; 0.138)	1.1e-13 *
cer.p	12.7-15.8 (14.2)	0.27-0.276 (0.674)	0.044 *
mt	12.3-15.8 (14)	0.295-0.302 (0.635)	0.0089 *
bg	11.3-13.6; 15.5-16.1; 18.6-19.6 (11.3; 15.5; 18.6)	0.333-0.339; 0.343-0.344; 0.348-0.349 (0.447; 0.0694; 0.104)	0.00011 *
thal	8.2-16.3 (8.2)	0.339-0.36 (0.771)	1.1e-08 *

For each region, the ages for stages of developmental change and age of peak change are reported, as are the range of the WM measure over the stage, rate of change and p value. Maturation time is defined as the time that the rate of change was no longer significantly different from the null (p=0.05, bootstrap corrected)

*significant after Holm correction within tract group/RTZs

#significant after Holm correction across all core tracts